Journal of Photochemistry and Photobiology A: Chemistry 217 (2011) 68–75

Contents lists available at ScienceDirect

Journal of Photochemistry and Photobiology A: Chemistry

journal homepage: www.elsevier.com/locate/jphotochem

Bubble-like CdSe nanoclusters sensitized TiO_2 nanotube arrays for improvement in solar cell

M.F. Hossain[a,b], S. Biswas[c], Z.H. Zhang[d], T. Takahashi[d,*]

[a] Graduate School of Science and Engineering for Education, University of Toyama, 3190 Gofuku, Toyama 930-8555, Japan
[b] Department of Electrical and Electronic Engineering, Rajshahi University of Engineering & Technology, Rajshahi 6204, Bangladesh
[c] LNM-IIT, Rupaki nangal, p.O-Sumel, Jaipur 302031, India
[d] Graduate School of Science and Engineering for Research, University of Toyama, 3190 Gofuku, Toyama 930-8555, Japan

ARTICLE INFO

Article history:
Received 24 May 2010
Received in revised form 17 August 2010
Accepted 25 September 2010
Available online 23 October 2010

Keywords:
Cadmium selenide
TiO_2 nanotubes
Nanoclusters
Solar cells

ABSTRACT

Solar cells were fabricated using novel bubble-like CdSe nanoclusters sensitized highly ordered titanium oxide nanotube (TiO_2 NT) array, prepared by anodization technique. The CdSe sensitization of TiO_2 NT arrays was carried out by a chemical bath deposition method with freshly prepared sodium selenosufite, ammonium hydroxide and cadmium acetate dehydrate at different deposition times: 20, 40 and 60 min. The adsorption of CdSe nanoclusters on the upper and inner surface of the TiO_2 NT arrays has been confirmed by field emission scanning electron and transmission electron microscopes. The results show the variation in cell a performance with different deposition times (20, 40, and 60 min) of CdSe on TiO_2 NT arrays. The solar cell with CdSe, deposited for 60 min, shows reasonably high photovoltaic property compared to the reported results of similar studies. This solar cell shows the maximum photoelectric conversion efficiency of 1.56% (photocurrent of 7.19 mA/cm^2; photovoltage of 0.438 V; and fill factor of 49.5%) and average incident photon to current efficiency of 50.2%. The photocurrent, incident photon-current efficiency and electron lifetime have been improved due to the increase of covered area and size of bubble-like CdSe nanoclusters on TiO_2 NT arrays with the increase of deposition time.

1. Introduction

The dye-sensitized solar cell (DSC) [1,2] has attracted a great deal of attention towards the next generation of solar cells due to its low production costs and high power conversion efficiency (~11%) [3]. The DSC is based on a wide band-gap semiconductor material with a very large internal surface to which dye molecules are attached [4]. Titanium oxide (TiO_2) is an important material in the construction of DSC, because of its suitable energy band position, and high photoelectric response as a porous photoelectrode material of DSC [1,4]. Morphology of TiO_2 films is important to improve the DSC efficiency. The tubular structure is the most suitable for nanostructures to achieve large enhancement in the surface area without increasing the geometric area. It is also suitable for unidirectional electron transfer [5]. Recently, Adachi et al. reported that the DSC with TiO_2 nanotube (TiO_2 NT) arrays showed more than double the photocurrent density of DSC with TiO_2 nanoparticles (P-25, thickness less than 5 μm) [6]. TiO_2 NT arrays have been fabricated by several methods, e.g., anodic oxidation [7], sol–gel [8], microwave irradiation [9], hydrothermal [10] and template synthesis [11]. Among these, anodic oxidation method is a relatively simple process for the fabrication of aligned TiO_2 NT arrays. Grimes and his coworkers [12] fabricated the first-generation TiO_2 NT arrays by electrochemical oxidation of titanium in an HF aqueous electrolyte with limited thickness (~500 nm). This technique has been further developed to obtain second-generation of highly ordered TiO_2 NT arrays with a high aspect ratio in organic electrolyte [13–16]. For the improvement of morphology, third-generation of TiO_2 NT arrays was introduced which requires water free electrolyte [17]. Recently, some research groups have succeeded to extend the length of TiO_2 NT arrays by using some polar organic electrolytes including formamide [14,18], ethylene glycol [14,19], dimethyl sulfoxide [14,19], and glycerol [20]. So, for this study, TiO_2 NT arrays have been prepared on Ti metal sheet by anodic oxidation method using ethylene glycol (EG) and NH_4F based electrolyte.

On the other hand, the photosensitizer plays an important role in determining the stability [21], light harvesting capability and also the total cost of the DSC. At present, despite the success of DSC using ruthenium dye [22], search for a cheaper alternative panchromatic sensitizer is still very relevant in order to improve the performance and reduce the cost of solar cell. Relatively short-band-gap semiconductors such as CdS [23], PbS [24], Bi_2S_3 [25], CdSe [26], and

* Corresponding author. Tel.: +81 76 445 6716; fax: +81 76 445 6716.
E-mail addresses: faruk94_ruet@yahoo.com (M.F. Hossain), takahash@eng.u-toyama.ac.jp (T. Takahashi).

1010-6030/$ – see front matter © 2010 Elsevier B.V. All rights reserved.
doi:10.1016/j.jphotochem.2010.09.020

InP [27] have been explored to serve as photosensitizer because of their advantages over dye that they can transfer electrons to large band gap semiconductor under visible light excitation and can tailor the nanocrystals through modification of solution growth method. Among these materials, nanocrystalline CdSe has a reasonably appropriate band gap (1.7 eV), which matches the solar-visible spectrum well and offers new opportunities to harvest light energy in the entire visible region of solar light. The nanocrystalline CdSe has been linked with TiO_2 NT arrays by a bi-functional molecule to improve the photoelectric conversion efficiency [28]. Recently, sensitization of mesoporous electrode by semiconductor quantum dot (QD) has also been studied [29]. Although CdSe QDs has more prospect than the larger CdSe nanoparticles those are not QD, but the power conversion efficiency of CdSe QDs sensitized solar cells is still not satisfactory [30]. The main reason for the low efficiency is the charge recombination process between photo-injected electrons and redox ions of the electrolyte [31]. CdSe nanoclusters can be very effective for their inexpensive and simple processing route [30]. Zhang et al. [32] have prepared the "mulberry-like" CdSe nanoclusters by using photo-assisted electrodeposition method, which exhibits strong potential in nanostructure devices. Nevertheless in their processing technique $Cd(NO_3)_2$ was used as a reactant which requires post-deposition annealing at 400 °C in N_2 atmosphere. Compared to Zhang et al. [32] and others synthesization techniques [33], we have been synthesized CdSe nanoclusters on TiO_2 NT arrays by inexpensive and simple chemical bath deposition (CBD) technique. These CdSe nanoclusters show the bubble-like structure of diameter 80–300 nm, which is a novel structure that can be prepared for the fabrication of solar cell without annealing it at any temperature. The bubble-like CdSe nanoclusters would be a promising nano-architecture to enhance the photoelectric conversion efficiency of the CdSe sensitized TiO_2 NT arrays due to its low recombination rate, high absorption and electron-hole separation in solar cells. The structural and surface morphological properties of bubble-like CdSe nanoclusters sensitized TiO_2 NT arrays and their photovoltaic performance were investigated and discussed.

2. Experimental procedures

In this work, CdSe nanoclusters sensitized TiO_2 NT arrays were successfully obtained by a low-cost and relatively simple two-step method. First, TiO_2 NT array were grown on a pure Ti-metal sheet via electrochemical anodic oxidation method in the EG and NH_4F based electrolyte and then CdSe nanoclusters were synthesized on the TiO_2 NT arrays through a CBD method.

2.1. Preparation of TiO_2 NT arrays

We used the anodic oxidation method to fabricate the TiO_2 NT arrays on Ti sheet. Prior to anodization, Ti sheet of 2.5 cm × 1.5 cm (99.6% purity, 0.2 mm thickness, Nilaco Co., Ltd., Tokyo, Japan) were first degreased by sonication in ethanol and cold distilled water in turn, followed by drying in a stream of pure nitrogen (N_2) flow. A conventional two-electrode system was employed with Ti foil as the anode and Pt foil as the cathode. The time-dependent behavior of the current under constant potential was recorded using a computer-controlled Keithley 2400 source-meter. All the anodization experiments were carried out at room temperature in an electrolyte of EG, 0.3 wt% of NH_4F and 3 vol% of water [14]. The exposed area of Ti sheet was 2 cm × 1.5 cm into the electrolyte, which anodized at 54 V for 45 min to obtain 5.7 μm thick nanotubes. After anodization, the sample was cleaned with EG and then distilled water, and it was dried with N_2 steam gas flow. The as-anodized TiO_2 NT arrays had an amorphous structure; they were subsequently crystallized by annealing in dry oxygen at 450 °C for 30 min with a heating and cooling rate of 2 °C/min.

2.2. Chemical bath deposition of CdSe nanoclusters on TiO_2 NT arrays

CdSe nanoclusters were deposited on aligned TiO_2 NT arrays by CBD method with different deposition times: 20, 40, and 60 min. At first, the sodium selenosulfite (Na_2SeSO_3) solution was prepared by dissolving of Se powder (99.999%, Aldrich) and sodium sulfite, Na_2SO_3 (Wako) in distilled water for 4 h at 65 °C. Undissolved Se was separated from the solution by filtration. After that 0.125 M of Na_2SeSO_3; 30 vol% of ammonium hydroxide, NH_4OH; and 0.5 M of cadmium acetate dehydrate, $Cd(CH_3COO)_2{\cdot}2H_2O$ are mixed with each other by using stirrer. The three TiO_2 NT arrays based substrates were immersed vertically in that solution. The bath-temperature was maintained at 90 °C during the CdSe deposition. The total deposition time was varied from 20 to 60 min.

The overall chemical reactions for the preparation of CdSe nanoclusters using CBD technique are given below:

$$Cd(NH_3)_4^{2+} + SeSO_3^{2-} + 2OH^- \rightarrow CdSe + 4NH_3 + SO_4^{2-} + H_2O \quad (1)$$

The chemical homogeneous equilibrium reaches through

$$Cd(NH_3)_4^{2+} \leftrightarrow Cd^{2+} + 4NH_3 \quad (2)$$

and

$$SeSO_3^{2+} + 2OH^- \leftrightarrow Se^{2-} + SO_4^{2-} + H_2O \quad (3)$$

which provides simultaneously slow and uniform generation of Cd^{2+} and Se^{2-} throughout the volume of the solution, allowing the deposition and growth of a CdSe films by ion-by-ion condensation:

$$Se^{2-} + Cd^{2+} \rightarrow CdSe \quad (4)$$

After 20, 40 and 60 min, the red CdSe coated TiO_2 NT arrays were removed from solution, respectively. The samples were gently rinsed with distilled water and dried in air. The crystal structure of the CdSe nanocluster sensitized TiO_2 NT arrays were examined by grazing incident X-ray diffraction (GIXRD) analysis with data collected from SHIMADZU XRD-6000 with Cu-Kα line. The data were recorded from 2θ values 10° to 80° with a step of 0.02°. For GIXRD measurement incident angle was fixed at 1.0°. The optical properties of the films were measured by SHIMADZU UV-vis NIR 3100 diffuse reflection spectrophotometer (DRS) at room temperature within the wavelength range 300–900 nm. The surface morphologies were studied using field emission scanning electron microscope (FE-SEM) (JEOL, FE-SEM 6700F) and transmission electron microscope (TEM, EM-002B, TOPCON Co. Ltd.). The chemical composition in wt% and compositional morphology was also estimated by energy dispersive spectroscopy (EDS, JED 2200) equipped with FE-SEM microscope. The CdSe inside the nanotube was also confirmed by the energy dispersive X-ray (EDX) attachment of TEM microscope.

2.3. Fabrication of CdSe sensitized solar cells

The CdSe sensitized solar cell has been assembled by placing bubble-like CdSe nanoclusters sensitized TiO_2 NT arrays face-to-face with a mildly platinum (~70 Å) coated SnO_2:F counter electrode as shown in the schematic diagram in Fig. 1(a). The two parallel electrodes were separated using spacer (SX1170-25) and clamped together. The space between the electrode (~20 μm) was filled by capillary force with the polysulfide electrolyte (2 M Na_2S and 3 M S (sulfur) dissolved in deionized water) [34]. The active cell area was 0.25 cm^2. The cell was irradiated by backside illumination with an artificial sunlight simulator, consisting of a SOLAX lamp (model: SET-140F, SERIC Ltd.) with ultraviolet and

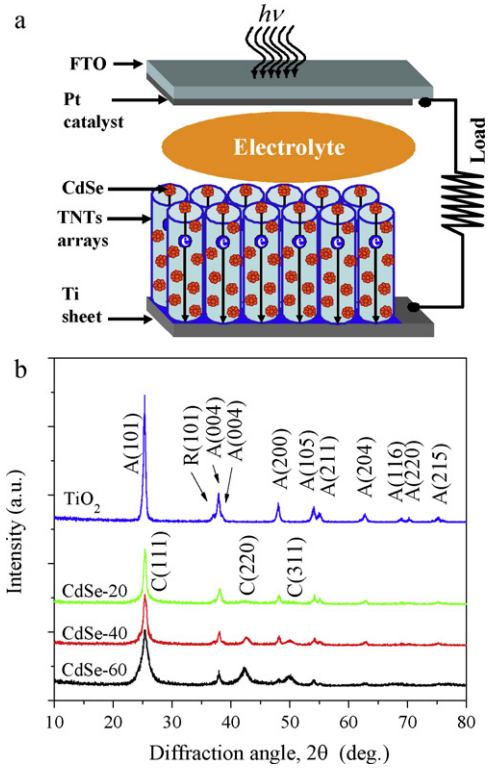

Fig. 1. (a) Schematic diagram of solar cells with bubble like CdSe sensitized TiO_2 NT arrays (b) the GIXRD pattern ($\alpha = 1.0^\circ$) of bare TiO_2 NT arrays and CdSe sensitized TiO_2 NT arrays at various deposition times of 20, 40, and 60 min.

an infrared-blocking filter. The intensity of light was 100 mW/cm^2. The photovoltaic measurements were performed using computer controlled Keithley Model-2400 source-meter unit and monochromator (SG-80, Yokogawa).

3. Results and discussion

Fig. 1(b) shows the GIXRD pattern (with incidence angle, $\alpha = 1.0^\circ$) of bare TiO_2 NT arrays and CdSe sensitized TiO_2 NT arrays with various CdSe-deposition times. The bare TiO_2 NT arrays have polycrystalline in nature with mostly anatase phase. Generally, CdSe nanoclusters deposited by CBD technique, has a polycrystalline wurtzite structure with highly preferential orientation. The CdSe sensitized TiO_2 NT arrays have single intensities C(1 1 1), C(2 2 0) and C(3 1 1) at 2θ values: 25.62°, 42.63° and 50.80°, respectively, which indicates a wurtzite (hexagonal) structure of CdSe (JCPDS card of 08-0459). The intensity of the peak of CdSe increases and TiO_2 NT arrays decreases with increase of deposition time, due to increase of amount of deposited material (CdSe). The crystallite size of the particles has been estimated from the Debye–Scherrer's equation as follows [35]: $D = 0.94\lambda/\beta\cos\theta$, where D is the crystallite size, λ is the wavelength of the X-ray radiation (Cu Kα = 0.15406 nm), θ is the diffraction angle and β is the full width half maximum. The diffraction peaks of A(1 0 1) and C(2 2 0) have been chosen for the calculation of the crystallite size. The derived crystallite sizes are 23.0, 8.64 and 5.4 nm for the bare TiO_2 NT arrays and CdSe nanoclusters 40 and 60 min, respectively.

The surface morphology of bare TiO_2 NT arrays was investigated by FE-SEM and TEM microscopes. Fig. 2(a), (b), and (c)–(e) show the top surface, bottom surface and cross-sectional view of the bare TiO_2 NT arrays, respectively. The average diameter of the nanotubes was 167 nm (±10 nm) with a wall thickness of 20 nm (±5 nm) and inner diameter 123 nm (±5 nm). The total length of the TiO_2 NT arrays is 5.7 μm [Fig. 2(e)]. The morphological properties were further investigated by using TEM image. Fig. 2(f) and (g) shows the top and cross-sectional view of a typical TEM image of the obtained bare TiO_2 NT arrays. The pore diameter of TiO_2 NT arrays is similar to the value, derived from FESEM image. The high-resolution TEM (HRTEM) image of the TiO_2 NT is shown in Fig. 2(h), from which the lattice fringe can be clearly observed, indicating good crystallization of these TiO_2 NT arrays. The d-spacing shows a value of

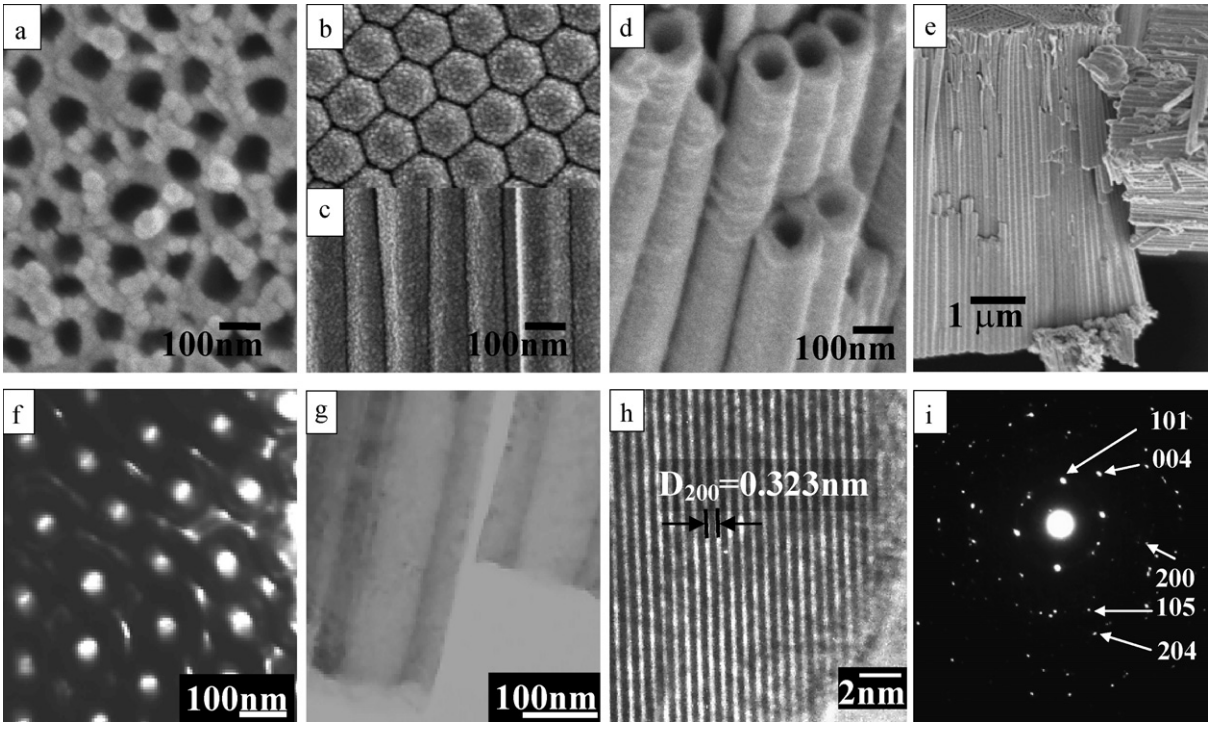

Fig. 2. The FE-SEM of bare TiO_2 NT arrays: (a) top, (b) bottom surface and (c)–(e) cross sectional view; and TEM image of bare TiO_2 NT arrays (f) top surface, (g) cross sectional view, (h) HRTEM image, and (i) SAED pattern.

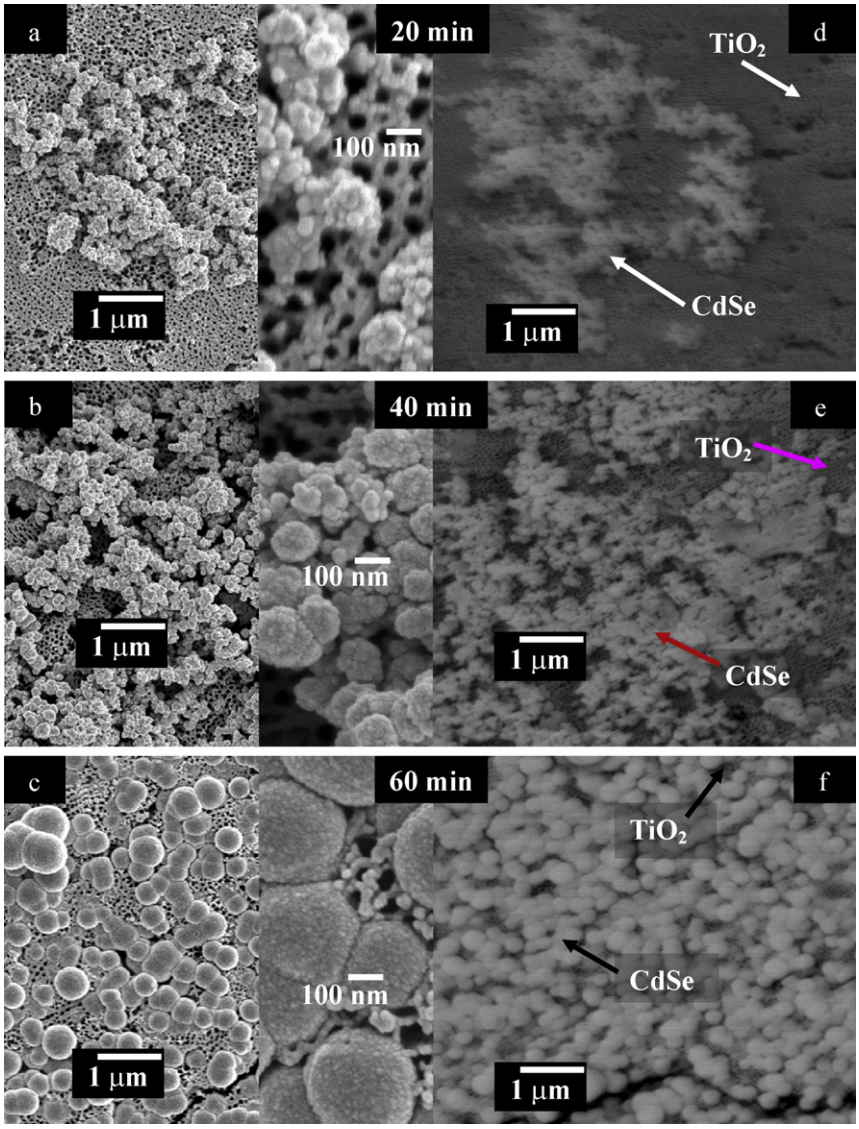

Fig. 3. (a–c) FE-SEM images of CdSe sensitized TiO_2 NT arrays and (d–f) compositional back scattering SEM images of CdSe sensitized TiO_2 NT arrays at various deposition times of 20, 40, and 60 min, respectively.

about 0.323 nm corresponds to anatase phase A(2 0 0) [36]. The corresponding selected area electron diffraction (SAED) pattern of bare TiO_2 NT arrays in anatase phases are shown in Fig. 2(i). These results are in agreement with the GIXRD results in Fig. 1(b). In this figure, the SAED patterns of TiO_2 NT arrays in anatase phase shows spotty ring patterns. From this figure, A(1 0 1), A(0 0 4), A(2 0 0), A(1 0 5), and A(2 0 4) peaks are confirmed [37].

The surface of the CdSe nanoclusters sensitized TiO_2 NT arrays with different deposition times: 20, 40 and 60 min are shown in Fig. 3(a)–(c), respectively. In Fig. 3(a), it has been observed that in the case of CdSe, deposited for 20 min, CdSe nonuniformly partially covers the TiO_2 NT surface. In this sample, size of the CdSe nanoparticle is around 15–25 nm. The amount of CdSe increases with the increase of deposition time. From Fig. 3(b), it is confirmed that the CdSe shows the 'Mulberry-like' structure [32] and tends to form bubble-like structure (80–110 nm). The structure of CdSe films absorbed on TiO_2 NT arrays (at 60 min) shows the bubble-like CdSe nanoclusters, shown in Fig. 3(c). It is confirmed from Fig. 3(b) and (c) that the bubble-like CdSe nanoclusters are successfully embedded into the TiO_2 NT arrays. For the bubble-like CdSe nanoclusters, secondary mono-disperse 3-D spheres formed from numerous primary nanocrystals. The CdSe for higher deposition time creates uniform cover on the TiO_2 NT surface which hides the surface of the TiO_2 NT arrays grains [38]. The average size of the bubble-like CdSe nanoclusters is 60–300 nm. These results are in good agreement with the back scattered FE-SEM images, given in Fig. 3(d)–(f). The quantitative analysis of the CdSe sensitized TiO_2 NT arrays were carried out by using the help of back scattered FE-SEM image. In these figures, the white objects are CdSe nanoclusters and dark part is TiO_2 NT surface. The CdSe nanoclusters have a tendency to cover the whole TiO_2 NT arrays surface with the increase of deposition time. In this context, it is important to be noted that the morphology of the TiO_2-nanotube structure has several advantages over TiO_2 nanoparticle structure for the following reasons. Vertically aligned TiO_2 nanotube with pore diameter ~60 nm ensure higher amount of CdSe deposition on inner TiO_2 surface. Moreover, for this nanotube structure, electrolyte can penetrate and come into the contact of CdSe surface even for sample of longer CdSe-deposition time.

The bubble-like CdSe nanoclusters inside the TiO_2 NT arrays are also confirmed by the TEM images, shown in Fig. 4. Fig. 4(a) shows the cross-sectional TEM image of CdSe nanoclusters sensitized TiO_2 NT arrays. It is confirmed that CdSe nanoclusters have been covered whole surface area (including inner surface) of TiO_2

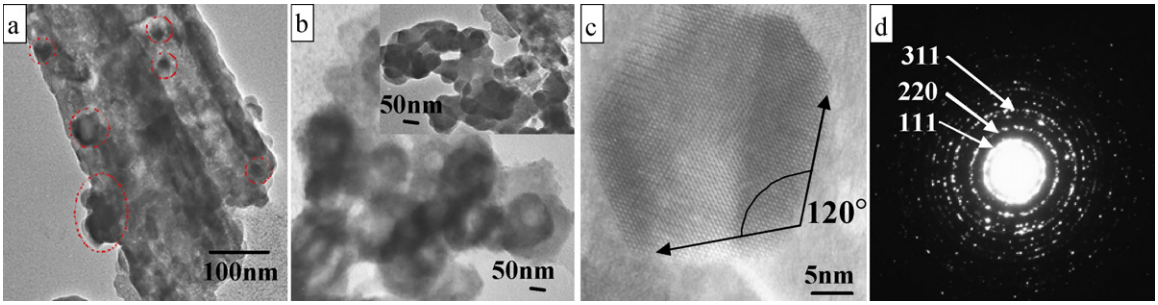

Fig. 4. TEM images of bubble like CdSe nanocluster sensitized TiO_2 NT arrays: (a) cross sectional view, red circle indicates the CdSe nanoclusters (b) bubble-like CdSe nanocluster, (c) HRTEM image of wurtzite CdSe nanocrystals, and (d) SAED pattern. (For interpretation of the references to color in this figure legend, the reader is referred to the web version of the article.)

NT arrays, which is marked with red circle. It also shows the bubble-like CdSe nanoclusters. Fig. 4(b) shows some bubble-like CdSe nanoclusters. The average diameter of the CdSe nanocluster is 100–300 nm, which supports the FE-SEM data. The HRTEM image of CdSe nanoclusters sensitized TiO_2 NT arrays is given in Fig. 4(c). It is confirmed that CdSe nanoclusters are wurtzite crystalline structure. The SAED pattern of CdSe nanocluster on the TiO_2 NT array shows the apparent ring diffraction patterns from the crystallinity of the wurtzite CdSe nanoclusters as well as spot diffraction patterns from the TiO_2 NT arrays [39]. It shows the C(1 1 1), C(2 2 0) and C(3 1 1) crystalline wurtzite phases.

Fig. 5 shows the typical EDS pattern (obtained from FE-SEM attachment) with relative analysis of CdSe nanoclusters sensitized TiO_2 NT arrays with 60 min. Since this is typically a surface measurement, the detected amount of Cd, Se increases and Ti, O decreases with increase of CdSe deposition time, shown in the (inset of Fig. 5) table. The Cd and Se are also confirmed inside the TiO_2 NT by EDX (attachment of TEM microscopy), shown in that mentioned table.

The incorporated amount of CdSe in TiO_2 NT arrays was evaluated using the absorbance of UV–vis spectrum. The absorption spectra corresponding to the bare TiO_2 NT arrays and CdSe nanoclusters sensitized TiO_2 NT arrays for different deposition times are shown in Fig. 6(a). The bare TiO_2 NT arrays show the absorption edge at 392 nm, which corresponds to 3.2 eV band gap. For the CBD process, the growth of CdSe on TiO_2 NT arrays is slow, which leads to low optical absorbance in inferred range. The optical absorbance increases slowly with increase of deposition time with slight red-shift of the absorption edge. For the CdSe sensitized TiO_2 NT arrays at 20 min, the band gap measured from the absorption edge (615 nm) is 1.952 eV, which is higher than the reported for CdSe (60 min) in bulk (714.3 nm, 1.73 eV). The transmittance of very thin (mildly) platinum is also shown in Fig. 6(a). The average transmittance of platinum is 46.34%, so the light can easily transfer through platinum counter electrode.

The effect of the sensitization on TiO_2 photoelectrode was probed by optical absorbance measurements in the wavelength range, 400–900 nm. Fig. 6(b) shows the difference of optical absorbance [(ΔA) = (absorbance of CdSe sensitized TiO_2 NT arrays) − (absorbance of bare TiO_2 NT arrays)] [38]. The effect of CdSe sensitization on TiO_2 NT arrays can be easily noticeable from the difference of absorbance (ΔA) spectrum, where a broad absorption peak, ranging from 400 to 615 nm has been observed. It indicates that in this specific wavelength range CdSe is more photoactive and mainly responsible for the electron generation. The ΔA

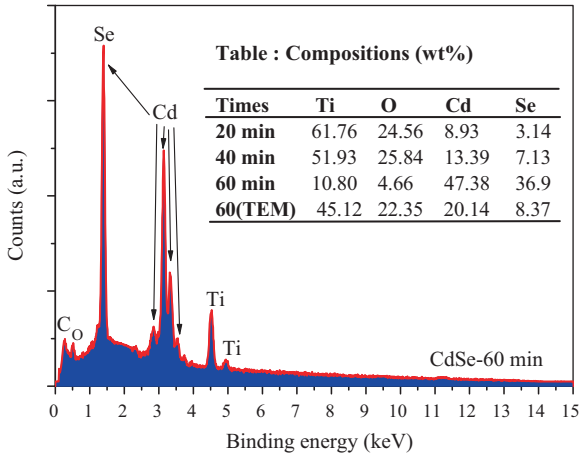

Table : Compositions (wt%)

Times	Ti	O	Cd	Se
20 min	61.76	24.56	8.93	3.14
40 min	51.93	25.84	13.39	7.13
60 min	10.80	4.66	47.38	36.9
60(TEM)	45.12	22.35	20.14	8.37

Fig. 5. EDS analysis of bubble-like CdSe sensitized TiO_2 NTs at 60 min deposition time. Table (inset): chemical composition of Ti, O, Cd and Se in wt% from FE-SEM and TEM (only 60 min sample) microscopes.

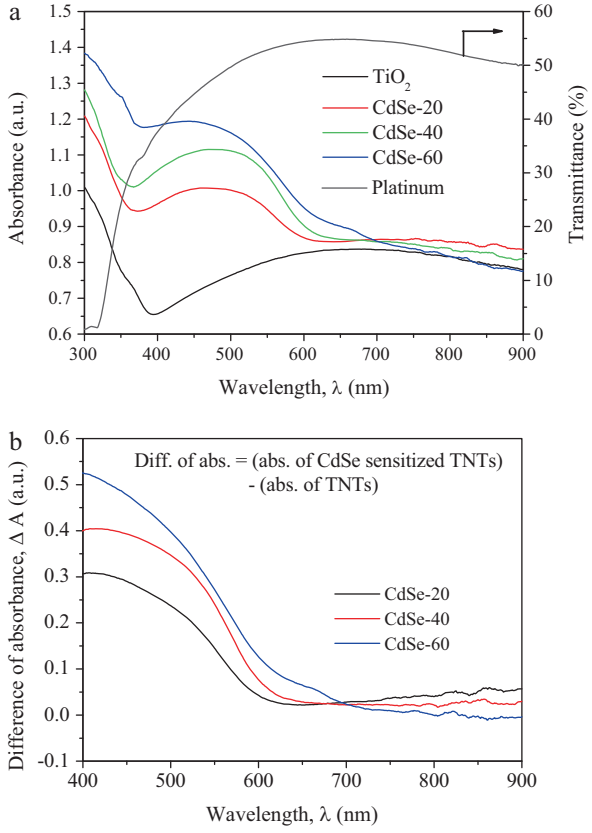

Fig. 6. (a) Absorbance spectra of TiO_2 NT arrays and CdSe sensitized TiO_2 NT arrays; and (b) difference of absorbance of TiO_2 NT arrays without and with CdSe sensitization at various deposition times of 20, 40, and 60 min.

Table 1
Photovoltaic performance of CdSe sensitize solar cells.

Deposition times (min)	V_{OC} (mV)	J_{SC} (mA/cm^2)	FF (%)	η (%)
20	383.0	4.08	52.1	0.81
40	425.2	5.2	51.0	1.13
60	438.0	7.19	49.5	1.56

spectrum of bubble-like CdSe sample prepared at 60 min, shows the higher value than the CdSe sample prepared at other deposition times. The difference of absorbance data has good agreement with the incident photon-to-current efficiency (IPCE) of solar cell.

Performance of the CdSe sensitized solar cells can be quantified on a macroscopic level in terms of IPCE, which gives the ratio between the number of generated charge carriers contributing to the photocurrent and the number of incident photons, as given by [40]:

$$IPCE\,(\%) = \left(\frac{1240 \times J_{SC}}{\lambda P_{in}}\right) \times 100\% \quad (5)$$

where J_{SC} is the photocurrent density, P_{in} is the intensity of the light, and λ is the wavelength of the incident light, respectively. The IPCE as a function of the wavelength of monochromatic irradiation is shown in Fig. 7(a). The average IPCE value of CdSe sensitized solar cell with 60 min sample is about 50.2% around the 400–570 nm. The IPCE spectrum shows two peaks, 61.5% and 48.3% at 446.5 and 528.3 nm, respectively. The position of these peaks is similar to CdSe absorbance, given in Fig. 6(b).

Another important parameter for a solar cell is its photoelectric conversion efficiency, i.e. the ratio of the output power to the incident power. The efficiency η of the CdSe sensitized solar cell can be calculated from the expression [41]:

$$\eta = \frac{J_{SC} V_{OC} FF}{P_{in}} \quad (6)$$

where J_{SC} is the integral photocurrent density, V_{OC} is the open-circuit voltage, and FF is the fill factor, $FF = (I \times V)_{max}/I_{SC}V_{OC}$. Fig. 7(b) shows the photocurrent–photovoltage characteristics of bubble-like CdSe nanoclusters sensitized solar cell in the 100 mW/cm^2 light illumination. The performance of the CdSe sensitized solar cells is summarized in Table 1. It is important to notice that the bubble-like CdSe nanoclusters sensitized solar cell at 60 min shows a maximum η of 1.56%, V_{OC} of 438 mV and J_{SC} of 7.19 mA/cm^2. The efficiency, photovoltage and photocurrent density decrease with decrease of CdSe deposition time. The CdSe sensitized solar cell at 20 min deposition shows η of 0.81%, V_{OC} of 383 mV and J_{SC} of 4.08 mA/cm^2, but it has the maximum fill factor of 52.1%. The fill factor decreases from 52.1% to 49.5% with increase of deposition time.

Fig. 7(c) shows the dark current characteristics of CdSe sensitized solar cell. We knew that the I_3^- could be penetrate into the porous inorganic semiconductor electrode, the electrons in conduction band of the n-type semiconductor could reduce the I_3^- to $3I^-$ at specific potential, which generates dark currents. This was illustrated in the following equations [42]:

$$2e_{cb}^-(TiO_2 \text{ or CdSe}) + I_3^- \xrightarrow{Ket[I_3^-]} 3I^- \quad (7)$$

In DSC, the recombination mainly involved in two processes: the photoinduced electrons recombined with the oxidized sensitizer and/or with I_3^- in the electrolyte. The dark current typically represents the recombination between the electrons in the conduction band and the I_3^-. In Fig. 7(c), the dark current of CdSe sensitized solar cell at 60 min is smaller than that of CdSe sensitized solar cells at 20 and 40 min. It is clearly indicates that the bubble-like CdSe nanoclusters sensitized solar cell improved both the charge-collection efficiency and the reduction of the charge recombination [32].

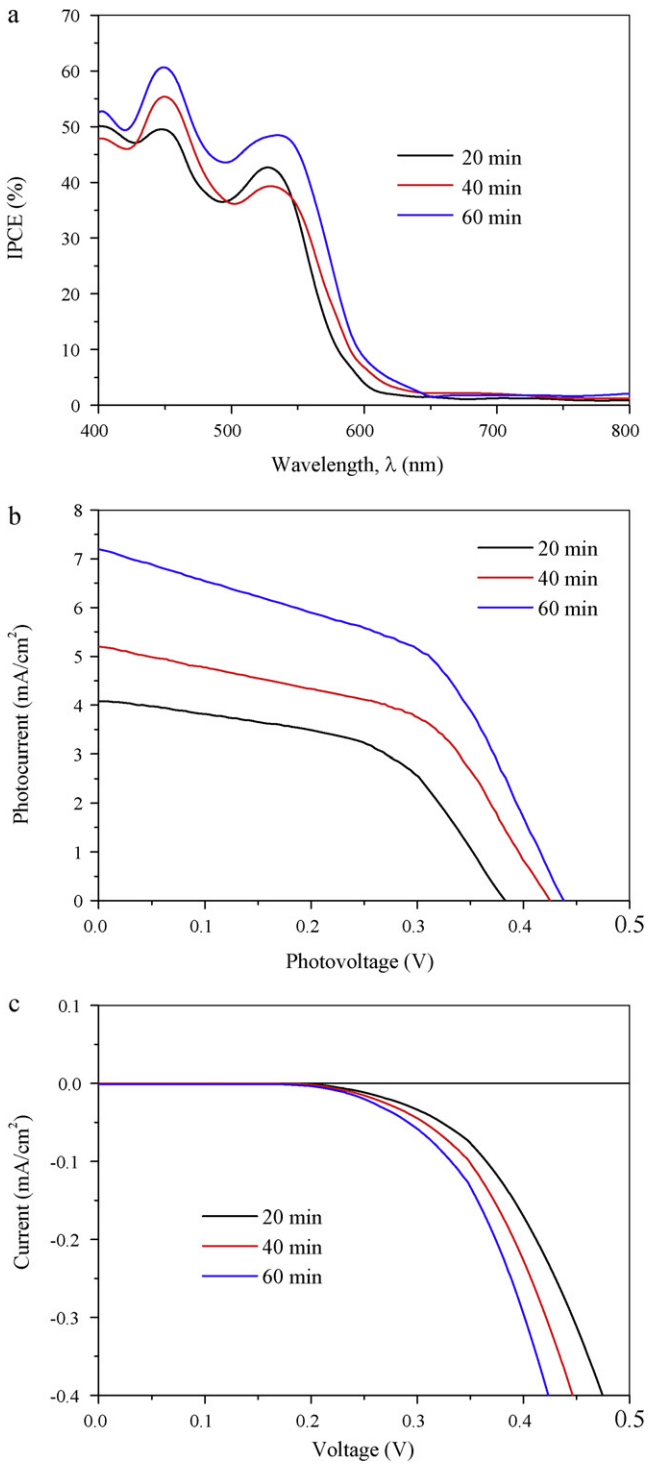

Fig. 7. (a) The IPCE spectra of bubble-like CdSe nanocluster sensitized solar cell; and I–V characteristics of bubble-like CdSe nanoclusters sensitized solar cell at various deposition times of 20, 40, and 60 min in: (b) 100 mW/cm^2 of light, and (c) dark condition.

Fig. 8(a) shows measurements of the rise and fall of the photocurrent during on–off cycles of light illumination (100 mW/cm^2). For both (rise and fall) cases, the time for changing the total photocurrent of solar cell at 60 min to 95% and more, is ~2.1 s faster than that of solar cell at other deposition times. Moreover, the CdSe layer on TiO_2 NT arrays is responsible for the faster response [43] due to a reduced recombination process. In the presence of a CdSe thin layer on TiO_2 NT arrays at 60 min, a 45% increment of photocurrent

Table 2
Comparative study of bubble-like CdSe nanoclusters sensitized solar cell with other CdSe sensitized solar cells, reported by some groups.

CdSe sensitizer	V_{OC}	J_{SC}	*FF*	η (%)	*IPCE* (%)	Reference
Bubble-like /TiO_2 NTs	438	7.19	49.5	1.56	50.2	Present study
Nanocrystals/ZnO nanorods	0.43	3.1		0.34		Tang et al. [21]
QDs/TiO_2 NTs/Ti	0.60	2.4		0.7	25	Kongkanaed et al. [28]
QDs/TiO_2 NPs/OTE	0.58	2.0		0.6	45	Kongkanaed et al. [28]
QDs/ZnO/TiO_2 NTs	0.67	2.73	0.58	1.07	36	Lee et al. [30]
QDs/TiO_2 NTs	0.64	2.33	0.56	0.85	28	Lee et al. [30]
QDs/TiO_2 NPs	0.63	1.88	0.58	0.69	25	Lee et al. [30]
QDs/TiO_2 films					30	Shen et al. [45]
QDs/ZnO nanorods	0.6	2.1		0.4	18	Leschkies et al. [46]
QDs/TiO_2 NP	0.61	3.15	0.61	1.17	36	Lee et al. [47]

is achieved compared to lower deposition time. The photocurrent increases with increase of deposition time. The on–off cycles of illumination further demonstrate the reproducibility and stability of the photocurrent response of CdSe nanoclusters sensitized solar cells.

Moreover, the photovoltage decay rate is directly related to the electron lifetime by the expression [44]:

$$\tau_n = \frac{-k_B T(dV_{OC}/dt)^{-1}}{e} \quad (8)$$

where the thermal energy is given by k_BT, e is the elementary charge, and dV_{OC}/dt is the derivative of the open circuit voltage transient. Fig. 8(b) is the plot of the response time obtained by applying this equation to the voltage decay (not shown). The CdSe nanoclusters sensitized solar cell at 20 min sample shows the shorter lifetime, but the bubble-like CdSe nanoclusters sensitized solar cell at 60 min sample exhibits superior recombination characteristics, with the longer lifetimes indicating lower recombination rate.

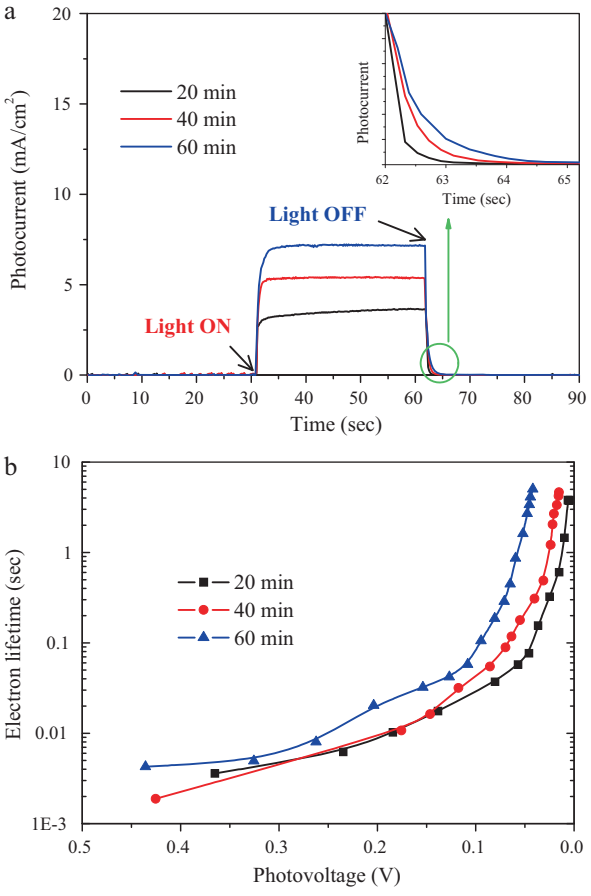

Fig. 8. (a) Photocurrent response of bubble-like CdSe nanoclusters sensitized solar cell, and (b) electron lifetime of these solar cells.

Table 2 shows the comparative photovoltaic performance of bubble-like CdSe nanoclusters sensitized solar cells with the solar cells which are already reported by some research groups [28,30,45–47]. The bubble-like CdSe nanoclusters sensitized solar cell has been showed better photovoltaic performance than the solar cells reported by others. The efficiency (1.56%) of bubble-like CdSe sensitized solar cells has been enhanced (~1.33 times) than other solar cells [21,28,30,45–47]. Comparing to other solar cells [21,28,30,45–47], the bubble-like CdSe nanoclusters sensitized solar cells shows more than double photocurrent density (7.19 mA/cm^2), which may be due to the bubble-like structures of CdSe nanoclusters. The photovoltage and FF are lower value due to use different electrolyte (2 M Na_2S and 3 M S). The average IPCE value, 50.2%, which is highest value among all solar cells reported in Table 2. So, bubble-like CdSe nanoclusters are more effective sensitizer to improve photoelectric conversion efficiency, photocurrent density, high charge separation and low recombination process and long lifetime from above discussion,

4. Conclusion

Highly aligned TiO_2 NT arrays were successfully synthesized on Ti sheet by using self-organized anodic oxidation method and TiO_2 NT arrays were sensitized with CdSe nanoclusters by CBD technique at different deposition times of 20, 40 and 60 min. This CBD technique ensure slow and uniform generation of Cd^{2+} and Se^{2-} throughout the volume of the solutions allowing the ion by ion growth mechanism which leads to novel bubble like structure. The bubble-like CdSe nanoclusters sensitized solar cells fabricated with deposition time 60 min shows the higher photoelectric conversion efficiency of 1.56%, IPCE of 50.2% and photocurrent density of 7.19 mA/cm^2 than the solar cells reported by the other groups. The electron lifetime has been improved in this solar cell that can be correlated to the higher surface coverage by the CdSe nanoclusters. However, the performance of bubble-like CdSe nanoclusters sensitized solar cells is still not very high, which is mainly due to the reduction of intensity of light for the case of backside illumination where light needs to pass through both the counter electrode and electrolyte.

Acknowledgement

Authors would like to thank to Mr. T. Kawabata, Materials Science and Engineering, University of Toyama, Japan for TEM measurement.

References

[1] B. O'Regan, M. Grätzel, A low-cost, high-efficiency solar cell based on dye-sensitized colloidal TiO_2 films, Nature 353 (1991) 737–740.
[2] M. Grätzel, Photoelectrochemical cells, Nature 414 (2001) 338–344.

[3] S. Ito, S.M. Zakeeruddin, R. Humphry-Baker, P. Liska, R. Charvet, P. Comte, M.K. Nazeeruddin, P. Péchy, M. Takata, H. Miura, S. Uchida, M. Grätzel, High-efficiency organic-dye-sensitized solar cells controlled by nanocrystalline-TiO_2 electrode thickness, Adv. Mater. 18 (2006) 1202–1205.
[4] M.F. Hossain, S. Biswas, T. Takahashi, Y. Kubota, A. Fujishima, Investigation of sputter-deposited TiO_2 thin film for the fabrication of dye-sensitized solar cells, Thin Solid Films 516 (2008) 7149–7154.
[5] Z.H. Zhang, Y. Yuan, G.Y. Shi, Y.J. Fang, L.H. Liang, H.C. Ding, L.T. Jin, Photoelectrocatalytic activity of highly ordered TiO_2 nanotube arrays electrode for azo dye degradation, Environ. Sci. Technol. 41 (2007) 6259–6263.
[6] M. Adachi, Y. Murata, I. Okada, S. Yoshikawa, Formation of titania nanotubes and applications for dye-sensitized solar cell, J. Electrochem. Soc. 150 (2003) G488–G493.
[7] G.K. Mor, O.K. Varghese, M. Paulose, C.A. Grimes, Transparent highly ordered TiO_2 nanotube arrays via anodization of titanium thin films, Adv. Funct. Mater. 15 (2005) 1291–1296.
[8] S.G. Yang, Y.Z. Liu, C. Sun, Preparation of anatase TiO_2/Ti nanotube-like electrodes and their high photoelectrocatalytic activity for the degradation of PCP in aqueous solution, Appl. Catal. A 301 (2006) 284–291.
[9] X. Wu, Q.Z. Jiang, Z.F. Ma, M. Fu, W.F. Shangguan, Synthesis of titania nanotubes by microwave irradiation, Solid State Commun. 136 (2005) 513–517.
[10] H.H. Ou, S.L. Lo, Review of titania nanotubes synthesized via the hydrothermal treatment: fabrication, modification, and application, Sep. Purif. Methods 58 (2007) 179–191.
[11] S.I. Na, S.S. Kim, W.K. Hong, J. Park, J. Jo, Y.C. Nah, T. Lee, D.Y. Kim, Fabrication of TiO_2 nanotubes by using electrodeposited ZnO nanorod template and their application to hybrid solar cells, Electrochim. Acta 53 (2008) 2560–2566.
[12] D. Gong, C.A. Grimes, O.K. Varghese, W. Hu, R.S. Singh, Z. Chen, E.C. Dickey, Titanium oxide nanotube arrays prepared by anodic oxidation, J. Mater. Res. 16 (2001) 3331–3334.
[13] A. Ghicov, H. Tsuchiya, J.M. Macak, P. Schmuki, Titanium oxide nanotubes prepared in phosphate electrolytes, Electrochem. Commun. 7 (2005) 505–509.
[14] M. Paulose, K. Shankar, S. Yoriya, H.E. Prakasam, O.K. Varghese, G.K. Mor, T.J. Latempa, A. Fitzgerald, C.A. Grimes, Anodic growth of highly ordered TiO_2 nanotube arrays to 134 μm in length, J. Phys. Chem. B 110 (2006) 16179–16184.
[15] H.E. Prakasam, K. Shankar, M. Paulose, C.A. Grimes, A new benchmark for TiO_2 nanotube array growth by anodization, J. Phys. Chem. C 111 (2007) 7235–7241.
[16] S.P. Albu, D. Kim, P. Schmuki, Growth of aligned TiO_2 bamboo-type nanotubes and highly ordered nanolace, Angew. Chem. Int. Ed. Commun. 47 (2008) 1916–1919.
[17] J.M. Macak, H. Tsuchiya, A. Ghicov, K. Yasuda, R. Hahn, S. Bauer, P. Schmuki, TiO_2 nanotubes: self-organized electrochemical formation, properties and applications, Curr. Opin. Solid State Mater. Sci. 11 (2007) 3–18.
[18] K. Shankar, G.K. Mor, A. Fitzgerald, C.A. Grimes, Cation effect on the electrochemical formation of very high aspect ratio TiO_2 nanotube arrays in formamide–water mixtures, J. Phys. Chem. C 111 (2007) 21–26.
[19] S. Yoriya, H.E. Prakasam, O.K. Varghese, K. Shankar, M. Paulose, G.K. Mor, T.J. Latempa, C.A. Grimes, Initial studies on the hydrogen gas sensing properties of highly-ordered high aspect ratio TiO_2 nanotube-arrays 20 μm to 222 μm in length, Sens. Lett. 4 (2006) 334–339.
[20] J.M. Macak, H. Tsuchiya, L. Taveira, S. Aldabergerova, P. Schmuki, Smooth anodic TiO_2 nanotubes, Angew. Chem. Int. Ed. 44 (2005) 7463–7465.
[21] Y. Tang, X. Hu, M. Chen, L. Luo, B. Li, L. Zhang, CdSe nanocrystal sensitized ZnO core–shell nanorod array films: preparation and photovoltaic properties, Electrochim. Acta 54 (2009) 2742–2747.
[22] M.K. Nazeeruddin, A. Kay, I. Rodicio, R. Humphry-Baker, E. Mueller, P. Liska, N. Vlachopoulos, M. Grätzel, Conversion of light to electricity by cis-X2bis(2,2′-bipyridyl-4,4′-dicarboxylate) ruthenium(II) charge-transfer sensitizers (X = Cl−, Br−, I−, CN−, and SCN−) on nanocrystalline titanium dioxide electrodes, J. Am. Chem. Soc. 115 (1993) 6382–6390.
[23] S. Biswas, M.F. Hossain, T. Takahashi, Fabrication of Grätzel solar cell with TiO_2/CdS bilayered photoelectrode, Thin Solid Films 517 (2008) 1284–1288.
[24] R. Plass, S. Pelet, J. Krueger, M. Grätzel, U. Bach, Quantum dot sensitization of organic–inorganic hybrid solar cells, J. Phys. Chem. B 106 (2002) 7578–7580.
[25] R. Vogel, P. Hoyer, H. Weller, Quantum-sized PbS, CdS, Ag_2S, Sb_2S_3, and Bi_2S_3 particles as sensitizers for various nanoporous wide-bandgap semiconductors, J. Phys. Chem. 98 (1994) 3183–3188.
[26] J.C. Lee, T.G. Kim, H.J. Choi, Y.M. Sung, Enhanced photochemical response of TiO_2/CdSe heterostructured nanowires, Cryst. Growth Des. 7 (12) (2007) 2589–2593.
[27] A. Zaban, O.I. Micic, B.A. Gregg, A.J. Nozik, Photosensitization of nanoporous TiO_2 electrodes with InP quantum dots, Langmuir 14 (1998) 3153–3156.
[28] A. Kongkanaed, K. Tvrdy, K. Takechi, M. Kuno, P.V. Kamat, Quantum dot solar cells. Tuning photoresponse through size and shape control of CdSe–TiO_2 architecture, J. Am. Chem. Soc. 130 (2008) 4007–4015.
[29] P.V. Kamat, Meeting the clean energy demand: nanostructure architectures for solar energy conversion, J. Phys. Chem. C 111 (2007) 2834–2860.
[30] W. Lee, S.H. Kang, J.Y. Kim, G.B. Kolekar, Y.E. Sung, S.H. Han, TiO_2 nanotubes with a ZnO thin energy barrier for improved current efficiency of CdSe quantum-dot-sensitized solar cells, Nanotechnology 20 (2009) 335706.
[31] S. Lee, J.Y. Kim, S.H. Youn, M. Park, K.S. Hong, H.S. Jung, J.K. Lee, H. Shin, Preparation of a nanoporous $CaCO_3$-coated TiO_2 electrode and its application to a dye-sensitized solar cell, Langmuir 23 (2007) 11907–11910.
[32] H. Zhang, X. Quan, S. Chen, H. Yu, N. Ma, "Mulberry-like" CdSe nanoclusters anchored on TiO_2 nanotube arrays: a novel architecture with remarkable photoelectrochemical performance, Chem. Mater. 21 (2009) 3090–3095.
[33] O. Niitsoo, S.K. Sarkar, C. Pejoux, S. Ruhle, D. Cahen, G. Hodes, Chemical bath deposited CdS/CdSe-sensitized porous TiO_2 solar cells, J. Photochem. Photobiol. A: Chem. 181 (2006) 306–313.
[34] M.F. Hossain, S. Biswas, T. Takahashi, Study of CdS-sensitized solar cells, prepared by ammonia-free chemical bath technique, Thin Solid Films 518 (2009) 1599–1602.
[35] B.D Cullity, Elements of X-ray Diffraction, Addison-Wesley, Reading, MA, USA, 1978.
[36] Y. Gao, S.A. Elder, TEM study of TiO_2 nanocrystals with different particle size and shape, Mater. Lett. 44 (2000) 228–232.
[37] L. Miao, S. Tanemura, S. Toh, K. Kaneko, M. Tanemura, Fabrication, characterization and Raman study of anatase-TiO_2 nanorods by a heating sol–gel template process, J. Cryst. Growth 264 (2004) 246–252.
[38] M.G.S. Paz, M.S. Lerma, A.M. Galvan, R.R. Bon, Optical properties and layer microstructure of CdS films obtained from an ammonia-free chemical bath deposition process, Thin Solid Films 515 (2007) 3356–3362.
[39] J.C. Lee, Y.M. Sung, T.G. Kim, H.J. Choi, TiO_2–CdSe nanowire arrays showing visible-range light absorption, Appl. Phys. Lett. 91 (2007) 113104.
[40] W.U. Huynh, J.J. Dittmer, A.P. Alivisatos, Hybrid nanorod–polymer solar cells, Science 295 (2002) 2425–2427.
[41] S.M. Sze, Physics of Semiconductor Devices, John Wiley & Sons, New York, 1981.
[42] W. Lee, J. Lee, S. Lee, W. Yi, S.-H. Han, B.W. Cho, Enhanced charge collection and reduced recombination of CdS/TiO_2 quantum-dots sensitized solar cells in the presence of single-walled carbon nanotubes, Appl. Phys. Lett. 92 (2008) 153510.
[43] K. Hara, Y. Dan-oh, C. Kasada, Y. Ohga, A. Shinpo, S. Suga, K. Sayama, H. Arakawa, Effect of additives on the photovoltaic performance of coumarin-dye-sensitized nanocrystalline TiO_2 solar cells, Langmuir 20 (2004) 4205–4210.
[44] G.K. Mor, K. Shankar, M. Paulose, O.K. Varghese, C.A. Grimes, Use of highly-ordered TiO_2 nanotube arrays in dye-sensitized solar cells, Nano Lett. 6 (2006) 215–218.
[45] Q. Shen, D. Arae, T. Toyoda, Photosensitization of nanostructured TiO_2 with CdSe quantum dots: effects of microstructure and electron transport in TiO_2 substrates, J. Photochem. Photobiol. A 164 (2004) 75–80.
[46] K.S. Leschkies, R. Divakar, J. Basu, E.E. Pommer, J.E. Boercker, C.B. Carter, U.R. Kortshagen, D.J. Norris, E.S. Aydil, Photosensitization of ZnO nanowires with CdSe quantum dots for photovoltaic devices, Nano Lett. 7 (2007) 1793–1798.
[47] H.J. Lee, J.H. um, H.C. Leventis, S.M. Zakeeruddin, S.A. Haque, P. Chen, S.I. Seok, M. Grätzel, M.K. Nazeeruddin, CdSe quantum dot-sensitized solar cells exceeding efficiency 1% at full-sun intensity, J. Phys. Chem. C 112 (2008) 11600–11608.